

14. G. S. Kwon. Polymeric micelles for delivery of poorly water-soluble compounds. *Crit. Rev. Ther. Drug Carr. Syst.* **20**:357-403 (2003).
15. G. Gaucher, M. H. Dufresne, V. P. Sant, N. Kang, D. Maysinger, and J. C. Leroux. Block copolymer micelles: preparation, characterization and application in drug delivery. *J. Control. Release* **109**:169-188 (2005).
16. H. Maeda. The enhanced permeability and retention (EPR) effect in tumor vasculature: the key role of tumor-selective macromolecular drug targeting. *Adv. Enzyme Regul.* **41**:189-207 (2001).
17. M. Yokoyama, T. Okano, Y. Sakurai, S. Fukushima, K. Okamoto, and K. Kataoka. Selective delivery of adriamycin to a solid tumor using a polymeric micelle carrier system. *J. Drug Target.* **7**:171-186 (1999).
18. K. Greish, T. Sawa, J. Fang, T. Akaike, and H. Maeda. SMA-doxorubicin, a new polymeric micellar drug for effective targeting to solid tumours. *J. Control. Release* **97**:219-230 (2004).
19. K. Kawano, M. Watanabe, T. Yamamoto, M. Yokoyama, P. Opanasopit, T. Okano, and Y. Maitani. Enhanced antitumor effect of camptothecin loaded in long-circulating polymeric micelles. *J. Control. Release* **112**:329-332 (2006).
20. T. Hamaguchi, Y. Matsumura, M. Suzuki, K. Shimizu, R. Goda, I. Nakamura, I. Nakatomi, M. Yokoyama, K. Kataoka, and T. Kakizoe. NK105, a paclitaxel-incorporating micellar nanoparticle formulation, can extend the therapeutic window of the drug. *Br. J. Cancer* **92**:1240-1246 (2005).
21. Y. Mizumura, Y. Matsumura, T. Hamaguchi, N. Nishiyama, K. Kataoka, T. Kawaguchi, W. J. Hrushesky, F. Moriyasu, and T. Kakizoe. Cisplatin-incorporated polymeric micelles eliminate nephrotoxicity, while maintaining antitumor activity. *Jpn. J. Cancer Res.* **92**:328-336 (2001).
22. S. Kawakami, P. Opanasopit, M. Yokoyama, N. Chansri, T. Yamamoto, T. Okano, F. Yamashita, and M. Hashida. Biodistribution characteristics of all-*trans* retinoic acid incorporated in liposomes and polymeric micelles following intravenous administration. *J. Pharm. Sci.* **94**:2606-2615 (2005).
23. P. Opanasopit, M. Yokoyama, M. Watanabe, K. Kawano, Y. Maitani, and T. Okano. Block copolymer design for camptothecin incorporation into polymeric micelles for passive tumor targeting. *Pharm. Res.* **21**:2001-2008 (2004).
24. M. Yokoyama, P. Opanasopit, T. Okano, K. Kawano, and Y. Maitani. Polymer design and incorporation methods for polymeric micelle carrier system containing water-insoluble anticancer agent camptothecin. *J. Drug Target.* **12**:373-384 (2003).
25. C. Managit, S. Kawakami, F. Yamashita, and M. Hashida. Effect of galactose density on asialoglycoprotein receptor-mediated uptake of galactosylated liposomes. *J. Pharm. Sci.* **94**:2266-2275 (2005).
26. K. Shimizu, K. Tamagawa, N. Takahashi, K. Takayama, and Y. Maitani. Stability and antitumor effects of all-*trans* retinoic acid-loaded liposomes contained sterylglucoside mixture. *Int. J. Pharm.* **258**:45-53 (2003).
27. G. Zuccari, R. Carosio, A. Fini, P. G. Montaldo, and I. Orienti. Modified polyvinylalcohol for encapsulation of all-*trans*-retinoic acid in polymeric micelles. *J. Control. Release* **103**:369-380 (2005).
28. Y. I. Jeong, M. K. Kang, H. S. Sun, S. S. Kang, H. W. Kim, K. S. Moon, K. L. Lee, S. H. Kim, and S. Jung. All-*trans*-retinoic acid release from core-shell type nanoparticles of poly(epsilon-caprolactone)/poly(ethylene glycol) diblock copolymer. *Int. J. Pharm.* **273**:95-107 (2004).
29. T. Takino, C. Nakajima, Y. Takakura, H. Sezaki, and M. Hashida. Controlled biodistribution of highly lipophilic drugs with various parenteral formulations. *J. Drug Target.* **1**:117-124 (1993).
30. Y. Hattori, S. Kawakami, F. Yamashita, and M. Hashida. Controlled biodistribution of galactosylated liposomes and incorporated probucol in hepatocyte-selective drug targeting. *J. Control. Release* **69**:369-377 (2000).
31. E. Ishida, C. Managit, S. Kawakami, M. Nishikawa, F. Yamashita, and M. Hashida. Biodistribution characteristics of galactosylated emulsions and incorporated probucol for hepatocyte-selective targeting of lipophilic drugs in mice. *Pharm. Res.* **21**:932-939 (2004).
32. K. Greish, J. Fang, T. Inutsuka, A. Nagamitsu, and H. Maeda. Macromolecular therapeutics: advantages and prospects with special emphasis on solid tumour targeting. *Clin. Pharmacokinet.* **42**:1089-1105 (2003).
33. N. Takahashi, K. Tamagawa, K. Shimizu, T. Fukui, and Y. Maitani. Effects on M5076-hepatic metastasis of retinoic acid and *N*-(4-hydroxyphenyl) retinamide, fenretinide entrapped in SG-liposomes. *Biol. Pharm. Bull.* **26**:1060-1063 (2003).
34. Y. Choi, S. Y. Kim, S. H. Kim, J. Yang, K. Park, and Y. Byun. Inhibition of tumor growth by biodegradable microspheres containing all-*trans*-retinoic acid in a human head-and-neck cancer xenograft. *Int. J. Cancer.* **107**:145-148 (2003).

Polymeric Micelles Modified by Folate-PEG-Lipid for Targeted Drug Delivery to Cancer Cells *In Vitro*

Akihiro Hayama¹, Tatsuhiro Yamamoto², Masayuki Yokoyama², Kumi Kawano¹,
Yoshiyuki Hattori¹, and Yoshie Maitani^{1,*}

¹Institute of Medicinal Chemistry, Hoshi University, 2-4-41 Ebara, Shinagawa-ku, Tokyo 142-8501, Japan

²Kanagawa Academy of Science and Technology, KSP East 404, Sakado 3-2-1, Takatsu-ku,
Kawasaki-shi, Kanagawa 213-0012, Japan

A novel technique was developed for the formation of ligand-targeted polymeric micelles that can be applicable to various ligands. For tumor-specific drug delivery, camptothecin (CPT)-loaded polymeric micelles were modified by folate to produce a folate-receptor-targeted drug carrier. Folate-linked PEG₅₀₀₀-distearoylphosphatidylethanolamine (folate-PEG₅₀₀₀-DSPE) was added when preparations of drug-loaded polymeric micelles, resulting in folate ligands exposed to the surface. Folate-modified CPT-loaded polymeric micelles (F-micelle) were evaluated by measuring cellular uptake using a flow cytometer, fluorescence microscopy, and confocal laser scanning microscopy, and by cytotoxicity measurement. The results revealed that F-micelle showed higher cellular uptake in KB cells over-expressing folate receptor (FR) and higher cytotoxicity compared with non-folate modified CPT-loaded polymeric micelles (plain micelles) in KB cells, but not in FR-negative HepG2 cells. This result indicated that polymeric micelles were successfully modified by the folate-linked lipid.

Keywords: Polymeric Micelles, Camptothecin, Targeting, Folate-PEG-Lipid, Folate.

1. INTRODUCTION

Camptothecin (CPT) has shown a broad spectrum of anti-tumor activity;^{1,2} however, its clinical use of CPT has some drawbacks, mainly due to water insolubility and aqueous instability of the lactone ring moiety. The lactone ring opens rapidly at physiological pH or above, resulting in a complete loss of biological activity.^{3,4}

Nanoparticles including polymeric micelles have attracted much attention in drug delivery research. Polymeric micelles are prepared from block copolymers possessing both hydrophilic and hydrophobic chains.^{5,6} Their advantageous characteristics for drug targeting include solubilization of hydrophobic molecules and high structural stability. CPT-loaded polymeric micelles enhanced the anticancer activity of CPT against solid tumors because of their prolonged blood circulation and higher accumulation in tumors.^{7,8}

As with other carriers, ligand-mediated targeting of polymeric micelles to target receptors expressed selectively or over-expressed on tumor cells is increasingly recognized as an effective strategy for improving the therapeutic effect of anticancer drugs. If CPT can

facilitate tumor targeting, a great contribution to the cancer chemotherapy is feasible. A variety of targeting ligands has been examined as tumor-targeted drug carriers. Folate receptor (FR) is abundantly expressed in a large percentage of human tumors, but it is only minimally distributed in normal tissue;⁹ therefore, FR can serve as a functional tumor-specific receptor. Folate modification of polymeric micelles has been reported to covalently conjugate block copolymer with folate.^{10,11} In these methods, the type of ligand must be decided in the preparation of polymeric micelles. In other words, the ligand-polymer conjugate must be synthesized with conformity to the drug. It is already known that a proper amount of folate-PEG-lipids could be inserted in liposomes and emulsions without change of their stability, and folate lipid-modified liposomes and emulsions with longer polyethylene glycol (PEG) linker were taken effectively by the FR-mediated cellular uptake.^{12,13} However, it has been no reports about surface-modified polymeric micelles by lipid. In polymer micelles, folate might not be able to be exposed outside by steric configuration of the hydrophilic block chain. Properties of the inner core such as hydrophobicity and rigidity, were very important to achieve micelles with stable drug incorporation.^{7,8,14} Folate lipid modification, therefore might affect the properties of the inner cores.

*Author to whom correspondence should be addressed.

For targeted drug delivery to cancer cells, we prepared folate-modified CPT-loaded polymeric micelles (F-micelle), and evaluated by measuring cellular uptake using a flow cytometer, fluorescence microscopy, and confocal laser scanning microscopy, and by cytotoxicity measurement. In this paper, we describe a novel method of folate modification to CPT-loaded polymeric micelles by folate-linked PEG₅₀₀₀-distearoylphosphatidylethanolamine (folate-PEG₅₀₀₀-DSPE).

2. MATERIALS AND METHODS

2.1. Materials

Poly(ethylene glycol)-poly(benzyl aspartate-53) block copolymer (PEG-P(Asp(Bz53))) was synthesized as described previously.^{14,15} The molecular weight of the PEG block was 2000 and the average number of aspartate units was 17. Fifty-three percentage of the aspartic acid residue was esterified with the benzyl group. CPT and folic acid were purchased from Wako Pure Chemicals (Tokyo, Japan). Folate-PEG₅₀₀₀-DSPE was synthesized as described previously.^{12,13} 1,1'-Diocadecyl-3,3,3',3'-tetramethylindocarbocyanine perchlorate (DiI) was purchased from Lambda Probes and Diagnostics (Graz, Austria).

2.2. Preparation of Folate-Modified CPT-Loaded Polymeric Micelles (F-Micelles)

CPT was incorporated into polymeric micelles by an evaporation method as described previously,¹⁵ using 0.5 mg of CPT, 5 mg of block copolymer, and 0 mol%, 0.03 mol% (0.027 mg), 0.1 mol% (0.092 mg) and 0.2 mol% (0.18 mg) of folate-PEG₅₀₀₀-DSPE to CPT loaded in micelles for plain micelles, 0.03F-micelle, 0.1F-micelle and 0.2F-micelle, respectively. DiI-labeled F-micelles were prepared by the same protocol, but with the post-addition of DiI at 0.4 mol% of incorporated CPT. The incorporation efficiency was calculated as described previously.¹⁵ The mean particle diameters and ζ -potentials were determined using a particle size analyzer (ELS-Z, Otsuka Electronics, Osaka, Japan) at 25 °C by diluting the dispersion to an appropriate volume with water.

2.3. *In Vitro* Drug Release

Release of CPT in F-micelles from a dialysis tube was measured using seamless cellulose tube membranes (Viskase Sales Corp., IL, USA) with a molecular cut-off of 12,000–14,000. The initial concentration of CPT was 10 μ g/ml. The sample volume in the dialysis bag was 1 ml and the sink volume was 200 ml PBS at pH 7.4 with the medium at 37 \pm 0.1 °C. The drug concentration was analyzed using fluorescence spectrophotometer F-4010 (Hitachi, Tokyo, Japan) (excitation 369 nm, emission 426 nm).

2.4. Cell Culture

KB cells (FR (+)) and HepG2 cells (FR (-)) were obtained from the Cell Resource Center for Biomedical Research, Tohoku University (Miyagi, Japan). Both cells were cultured in folate-deficient RPMI 1640 medium (Invitrogen Corp., Carlsbad, CA, USA) with 10% heat-inactivated fetal bovine serum (Invitrogen Corp.) and 100 μ g/ml kanamycin with 5% CO₂ at 37 °C.

2.5. Flow Cytometry Analysis

KB cells were prepared by plating 5 \times 10⁵ cells in a 6-well culture plate 1 day before the assay. Cells were incubated with DiI-labeled F-micelles containing 10 μ g CPT/ml diluted in 2 ml folate-deficient RPMI 1640 medium for 2 hours at 37 °C. In free-folic acid competition studies, 2 mM folic acid was added to the medium. After incubation, cells were washed two times with acidic saline (pH 3) followed by one wash with cold phosphate-buffered saline (PBS, pH 7.4) to remove unbound polymeric micelles, detached with 0.02% EDTA-PBS, and then suspended in PBS containing 0.1% bovine serum albumin and 1 mM EDTA. The suspended cells were directly introduced to a FACSCalibur flow cytometer (Becton Dickinson, San Jose, CA, USA) equipped with a 488 nm argon ion laser. Data for 10,000 fluorescent events were obtained by recording forward scatter, side scatter, and 585/42 nm fluorescence. The autofluorescence of cells was taken as a control.

2.6. Fluorescence and Confocal Laser Scanning Microscopy

After incubation, cells were washed as described above; 2 ml fresh medium was added. The cells were observed with fluorescence microscopy (ECLIPSE TS100, Nikon, Tokyo, Japan) at just. For confocal laser scanning microscopy, cells were fixed with Mildform 20 N for 30 min at room temperature. Subsequently, the cells were washed three times with PBS. Examinations were performed with a Radiance 2100 confocal laser-scanning microscope (BioRad, CA, USA).

2.7. Cytotoxicity Study

Cells were prepared by plating 1 \times 10⁴ cells in a 96-well culture plate 1 day before the experiment. KB and HepG2 cells were then incubated for 2 hours at 37 °C with 100 μ l CPT solution, plain micelle, and F-micelles (containing 0.01, 0.1, 0.5, 1, 2.5 and 5 μ g CPT) diluted in folate-deficient RPMI 1640 medium. The medium was replaced with fresh medium and incubated for a further 48 hours. Cytotoxicity was determined with the WST-8 assay (Dojindo Laboratories, Kumamoto, Japan). The number of viable cells was then determined by absorbance measured at 450 nm on an automated plate reader (BioRad, CA, USA).

2.8. Statistical Analysis

Statistical comparisons were performed by Student's *t*-test. *P* values less than 0.05 were considered significant.

3. RESULTS AND DISCUSSION

3.1. Determination of CPT Content and Particle Size of F-Micelles

In our previous study, folate modification with a sufficiently long PEG chain on emulsion is an effective way of targeting drug carriers to tumor cells.¹³ Therefore, folate-lipid conjugate with PEG₅₀₀₀ linker was used for the modification of polymeric micelles with PEG₂₀₀₀. Four kinds of CPT-loaded polymeric micelles were formulated as plain micelles, 0.03F-micelle, 0.1F-micelle and 0.2F-micelle. Folate-PEG-DSPE may be incorporated to polymeric micelles since 0.2 mol% folate-PEG₅₀₀₀-DSPE was 9.6 μ M, and the critical micelle concentration (CMC) value of folate-PEG₅₀₀₀-DSPE was 12.1 μ M determined by the fluorescence probe technique using DiI.

The average particle size of each F-micelle in water was about 230 nm with 0.5–1.1 mV in ζ -potential and the CPT-loading efficiency was about 50%. These values of F-micelles did not change significantly compared with plain micelles.

3.2. *In Vitro* Drug Release

The *in vitro* release of CPT from 0.03F-micelle exhibited rapid release behavior in an early stage (about 40% in 2 hours, Fig. 1). In contrast, the release of CPT from 0.2F-micelle and plain micelles reached only about 20% after the same period of incubation. This result indicates that the quantity of folate modification affected the stability of polymeric micelles, indicating that the higher the

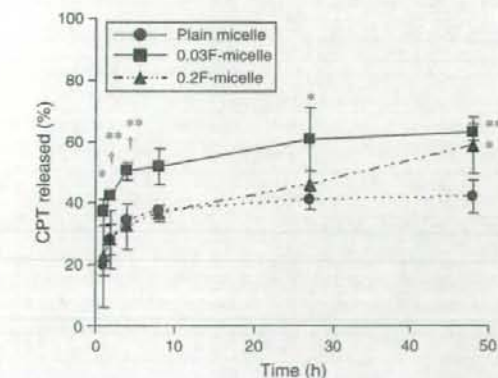


Fig. 1. Release profiles from plain and folate-modified CPT-loaded polymeric micelles at 37 °C in PBS as a sink solution at pH = 7.4. Each value represents the mean \pm S.D. (*n* = 3). **P* < 0.05, ***P* < 0.01 compared with plain micelle, †*P* < 0.05 compared with 0.2F-micelle.

folate surface density, the lower the drug release. Similar results were reported that folate modification of liposomes influenced the release pattern.¹⁶ The decreased drug release from highly folate-modified polymer micelles might be due to the structural integrity of folate coupling, that may lead to barrier effect for CPT diffusion.

3.3. Uptake of F-Micelles to KB Cells

Cellular uptake of F-micelle was evaluated using polymeric micelles labeled with DiI by flow cytometry. The fluorescence of 10 μ g CPT/ml of DiI-labeled plain

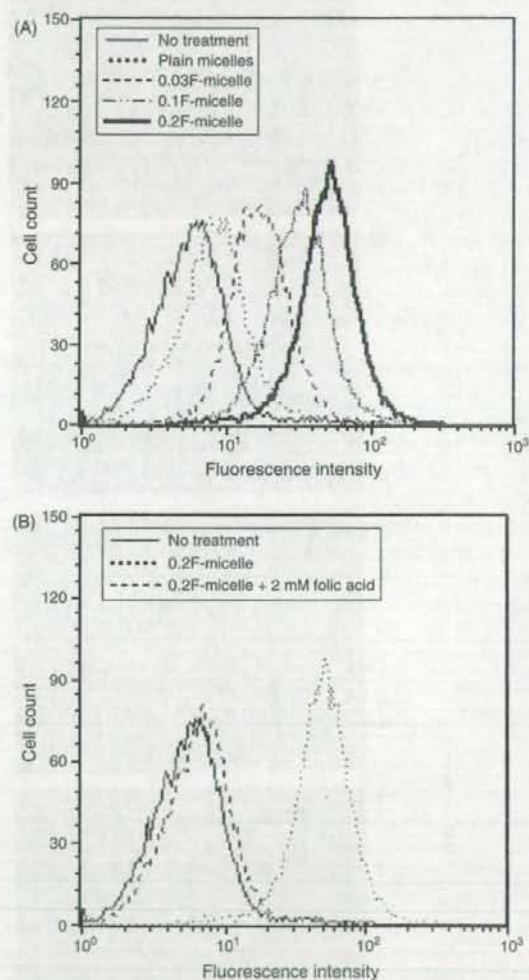


Fig. 2. Uptake of DiI-labeled plain and folate-modified CPT-loaded polymeric micelles with KB cells in the absence (A), or presence of 2 mM folic acid (B). Cells were incubated with polymeric micelles in folate-free RPMI 1640 medium for 2 hours at 37 °C and analyzed by flow cytometry. No treatment indicates autofluorescence of untreated cells. Each analysis was generated by counting 10⁴ cells.

micelles and F-micelles showed almost identical spectrofluorimetric units (data not shown). As shown in Figure 2(A), flow cytometry analysis represented a shift in the curve. 0.2F-micelle indicated higher mean intensity of about 13.8-fold, 7.9-fold and 3.3-fold in cellular association of plain micelles, 0.03F-micelle and 0.1F-micelle after 2 hours exposure, respectively. In contrast, micelles modified with methoxy-PEG₅₀₀₀-DSPE showed a similar curve to plain micelles (data not shown). Additionally, these increased associations of 0.03F-micelle, 0.1F-micelle (data

not shown) and 0.2F-micelle could be completely blocked by adding 2 mM folic acid to the medium (Fig. 2(B)). This is the first report showing that folate-lipid was incorporated and its folate group was exposed on the surface of polymeric micelles to interact with FR. The results also indicate that F-micelle was transported within cells by an FR-mediated endocytosis process. These findings are consistent with those reported previously on the FR-mediated cellular uptake of folate-modified liposomes and emulsions for anti-cancer therapy.^{12,13}

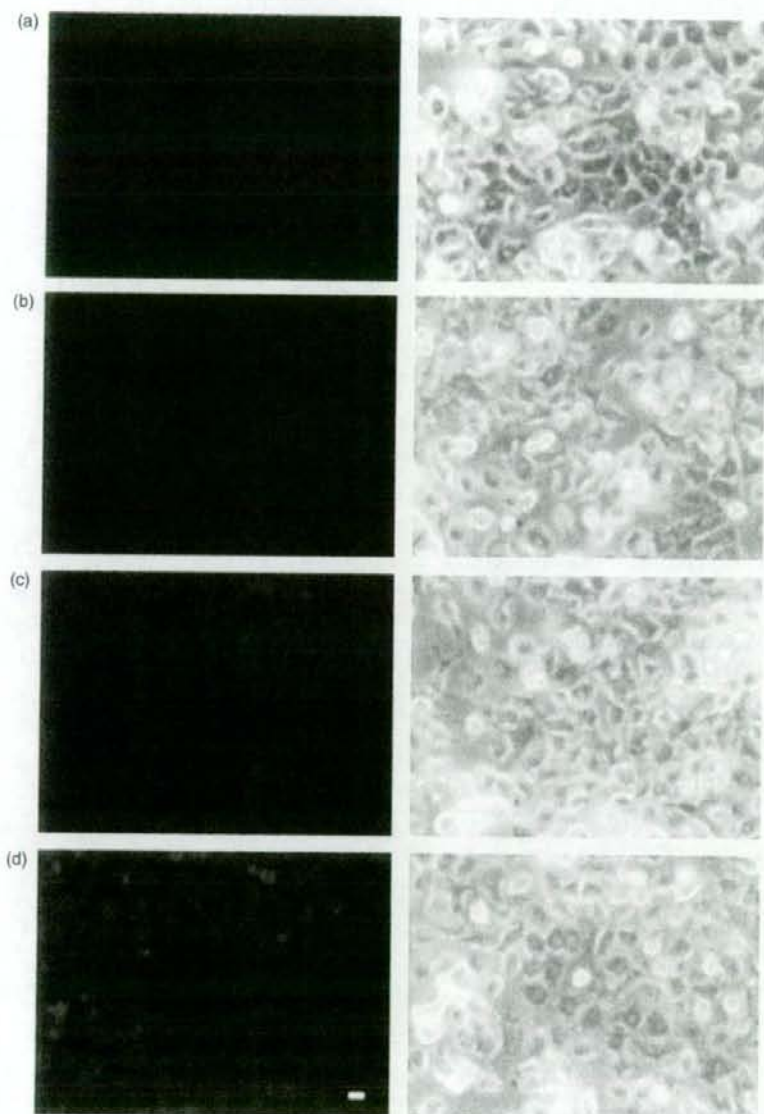


Fig. 3. Fluorescence microscopic images of KB cells treated with (a) plain micelles, (b) 0.03F-micelle, (c) 0.1F-micelle and (d) 0.2F-micelle. Cells were incubated with polymeric micelles in folate-free RPMI 1640 medium for 2 hours at 37 °C, then observed just after. ($\times 200$) Scale bar denotes 10 μm .

Cellular uptake of F-micelles was also evaluated using fluorescence microscopy. Fluorescence images of KB cells after incubation with F-micelles for 2 hours are shown in Figure 3. For plain micelles, there was no remarkable uptake in fluorescent intensity of KB cells. In contrast, in F-micelles, more fluorescently labeled cells could be clearly visualized, and 0.2F-micelle was especially taken up in to the cells. This result is similar to that of flow cytometry. In accordance with the results from flow cytometry analysis, fluorescence microscopy confirmed that F-micelles could be targeted to cancer cells over-expressing FR on their surface.

3.4. Localization of F-Micelles to KB Cells

To investigate whether F-micelles existed on cell surface or within cells, localization of F-micelles was evaluated using confocal laser scanning microscopy. Fluorescence images of KB cells after incubation with 0.03F-micelle for 2 hours are shown in Figure 4. 0.2F-micelle showed similar image (data not shown). The localization of DiI-labeled

F-micelles was confirmed by changing the Z-axis of observed area with 1 μm . DiI-fluorescence was detected as punctuate dots within cells. This indicated that F-micelles were internalized into the cells and located within endosome compartments.

3.5. Cytotoxicity Study

FR-targeted polymeric micelles were evaluated for *in vitro* cytotoxicity in FR (+) KB and FR (-) HepG2 cells by WST-8 assay. Superior cytotoxicity of F-micelles over plain micelles was observed in KB cells, but not in HepG2 cells. IC_{50} values for KB cells of F-micelles were about 2–3 times lower than the plain micelles (Table I). The difference of IC_{50} values between 0.03F-micelle and 0.2F-micelle was not large. It might be due to the release of CPT from 0.03F-micelle was faster than that from 0.2F-micelle, and free CPT was taken up to the cells as well as micelles. In contrast, IC_{50} values for HepG2 cells show hardly any difference between F-micelles and plain micelles.

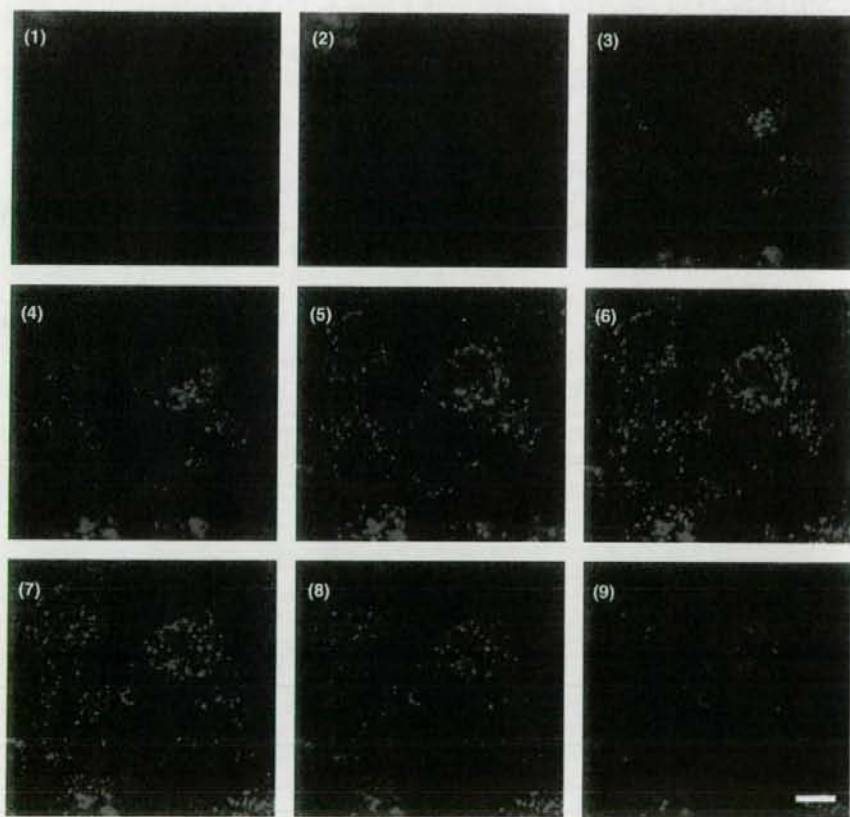


Fig. 4. Localization of DiI-labeled folate-modified CPT-loaded polymeric micelles (0.03F-micelle) with KB cells. Cells were incubated with polymeric micelles in folate-free RPMI 1640 medium for 2 hours at 37 °C, then observed just after under confocal laser scanning microscopy by changing the Z-axis. Images (1–9) represent regular intervals of 1 μm on the Z-axis from bottom to top cells, respectively. ($\times 1200$) Scale bars denote 10 μm .

Table I. IC₅₀ value (μg/ml) of CPT solution, plain micelles, folate-modified CPT-loaded polymeric micelles for KB cells and HepG2 cells.

Cells	CPT-solution	Polymeric micelles			
		Plain	0.03F	0.1F	0.2F
KB	3.0 ± 0.4	6.7 ± 1.1	2.2 ± 0.5	3.6 ± 0.8	2.1 ± 0.9
HepG2	2.2 ± 0.2	8.7 ± 0.9	8.4 ± 0.4	7.4 ± 1.0	6.5 ± 1.6

Data are shown as the mean ± S.D. (n = 3).

The CPT lactone ring opened at about 20 minutes in medium.³ The lactone E-ring in CPT plays an important role in a drug's biological activity but it exists in a pH-dependent equilibrium in an open ring carboxylate form. Incorporation of CPT in micelles could maintain active lactone form even in the presence of serum,¹⁴ indicating that micelle formulations could keep the antitumor effect of CPT. Plain micelles showed lower cytotoxicity than CPT solution, because the PEG shells of polymeric micelles inhibited interaction with cells. However, folate modification of polymeric micelles increased the association with cells via FR, resulting in increase of the cytotoxicity similar to CPT solution. It is one of the reasons that IC₅₀ values of F-micelles were much higher or similar to those for CPT solution. Preferential partitioning of the lactone form into lipid layers has been previously reported to stabilize CPT.^{3,17} *In vivo* situation, micelle formulation enhanced the accumulation in tumor tissue than CPT solution.⁸ Further interaction of folate may increase the antitumor effect of CPT micelles. These results indicate that 0.2F-micelle is suitable drug carrier for selective drug delivery and is more adapted than 0.03F-micelle.

4. CONCLUSION

Uptake and cytotoxicity study showed that F-micelles could be selectively taken into cancer cells by folate-receptor mediated endocytosis. The novel lipid-based modification method to polymeric micelles is applicable to antibody, peptides, or other ligands. Furthermore, this allows double targeting using folate-lipid and another

ligand-conjugated polymeric micelles or folate-targeted therapeutics to be tailored to the needs of individual patients.

Acknowledgments: This work was supported by Grants-in-Aids from the Ministry of Health, Labour and Welfare of Japan, and by Open Research Center Project. We are grateful to Mr. Atsushi Yamada and Mr. Takashi Yoshizawa for providing folate-PEG₅₀₀₀-DSPE.

References and Notes

- B. C. Giovanella, H. R. Hinz, A. J. Kozielski, J. S. Stehlin, Jr., R. Silber, and M. Potmesil, *Cancer Res.* 51, 3052 (1991).
- B. C. Giovanella, J. S. Stehlin, M. E. Wall, M. C. Wani, A. W. Nicholas, L. F. Liu, R. Silber, and M. Potmesil, *Science* 246, 1046 (1989).
- T. G. Burke, A. E. Staubus, and A. K. Mishra, *J. Am. Chem. Soc.* 114, 8318 (1992).
- J. Fassberg and V. J. Stella, *J. Pharm. Sci.* 81, 676 (1992).
- K. Kataoka, A. Harada, and Y. Nagasaki, *Adv. Drug Deliv. Rev.* 47, 113 (2001).
- V. P. Torchilin, *Mol. Life Sci.* 61, 2549 (2004).
- M. Watanabe, K. Kawano, M. Yokoyama, P. Opanasopit, T. Okano, and Y. Maitani, *Int. J. Pharm.* 308, 183 (2006).
- K. Kawano, M. Watanabe, T. Yamamoto, M. Yokoyama, P. Opanasopit, T. Okano, and Y. Maitani, *J. Control. Release* 112, 329 (2006).
- M. Wu, M. Gunning, and M. Ratnam, *Biomarkers Prev.* 8, 775 (1999).
- P. V. Paranjpe, Y. Chen, V. Kholodovych, W. Welsh, S. Stein, and P. J. Sinko, *J. Control. Release* 100, 275 (2004).
- H. S. Yoo and T. G. Park, *J. Control. Release* 96, 273 (2004).
- A. Gabizon, A. T. Horowitz, D. Goren, D. Tzemach, F. Mandelbaum-Shavit, M. M. Qazen, and S. Zalipsky, *Bioconjug. Chem.* 10, 289 (1999).
- T. Shiokawa, Y. Hattori, K. Kawano, Y. Ohguchi, H. Kawakami, K. Toma, and Y. Maitani, *Clin. Cancer Res.* 11, 2018 (2005).
- P. Opanasopit, M. Yokoyama, M. Watanabe, K. Kawano, Y. Maitani, and T. Okano, *Pharm. Res.* 21, 2001 (2004).
- M. Yokoyama, P. Opanasopit, T. Okano, K. Kawano, and Y. Maitani, *J. Drug Target.* 12, 373 (2004).
- Y. Gupta, A. Jain, P. Jain, and S. Jain, *J. Drug Target.* 15, 231 (2007).
- Y. Sadzuka, S. Hirotsu, and S. Hirota, *Jpn. J. Cancer Res.* 90, 226 (1999).

Received: 20 June 2007. Accepted: 8 August 2007.



Note

Block copolymer design for stable encapsulation of *N*-(4-hydroxyphenyl)retinamide into polymeric micelles in mice

Tomoyuki Okuda^a, Shigeru Kawakami^a, Masayuki Yokoyama^b, Tatsuhiro Yamamoto^b,
Fumiyoshi Yamashita^a, Mitsuru Hashida^{a,*}

^a Department of Drug Delivery Research, Graduate School of Pharmaceutical Sciences,
Kyoto University, Sakyo-ku, Kyoto 606-8501, Japan

^b Kanagawa Academy of Science and Technology, KSP East 404, Sakado 3-2-1, Takatsu-ku,
Kawasaki-shi, Kanagawa 213-0012, Japan

Received 5 October 2007; received in revised form 22 January 2008; accepted 24 January 2008

Abstract

For stable encapsulation of *N*-(4-hydroxyphenyl)retinamide (4-HPR) into polymeric micelles, four types of block copolymers were synthesized with different esterified functional groups: heptyl (C7), nonyl (C9), benzyl (Bz), and phenylpropyl (C3Ph). The stability of 4-HPR encapsulated polymeric micelles was evaluated by measuring the blood concentration of 4-HPR in mice. After intravenous administration of 4-HPR and 4-HPR encapsulated PEG liposomes, the blood concentration of 4-HPR was about 2.8% and 2.2% of the dose/mL, suggesting the rapid release of 4-HPR from PEG liposomes. In contrast, the blood concentration of 4-HPR after intravenous administration of all 4-HPR encapsulated polymeric micelles studied was much higher (about 22–34% of the dose/mL). Among them, the polymeric micelles prepared by block copolymers (Bz) showed the highest blood concentration of 4-HPR. As far as the effects of the level of Bz groups in the block copolymers are concerned, the blood concentration of 4-HPR was enhanced by Bz groups at a level of 72% and 77%, but not by Bz groups at a level of 43% and 51%. These results suggest that 4-HPR is stably encapsulated in polymeric micelles prepared by block copolymers (Bz) but a level of over 72% of Bz groups is needed. These findings will be of value in the future use, design, and development of polymeric micelles for *in vivo* application of 4-HPR.
© 2008 Elsevier B.V. All rights reserved.

Keywords: 4-HPR; Fenretinide; Polymeric micelle; Controlled release; Drug delivery systems

N-(4-Hydroxyphenyl)retinamide (4-HPR, fenretinide) is a synthetic retinoid which shows high anti-tumor activity against a variety of malignant cells (Formelli et al., 1996). Although oral administration of 4-HPR has been used in clinical trials so far, its bioavailability is very limited because of its low membrane permeability (Kokate et al., 2006). In addition, intravenous 4-HPR is rapidly eliminated from body (Swanson et al., 1980; Hultin et al., 1986). Therefore, 4-HPR cannot exert a high enough anti-tumor activity because its low blood concentration (Formelli et al., 1993). Raffaghello et al. and Takahashi et al. have reported that 4-HPR encapsulated liposomes containing monoclonal antibody or sterylglucoside mixture exert anti-tumor activities when given intravenously. Therefore, the development of a targeting carrier for 4-HPR is needed in order to obtain potent *in vivo*

anti-tumor activity (Raffaghello et al., 2003; Takahashi et al., 2003).

Polymeric micelles prepared by block copolymers, which are composed of both hydrophilic and hydrophobic segments, have been reported to be suitable drug carriers for lipophilic drugs (Kataoka et al., 2001; Gaucher et al., 2005). Recently, we have reported the efficient encapsulation of hydrophobic drugs in polymeric micelles by optimizing the hydrophobic segments with esterified functional groups of poly(ethylene glycol)-poly(aspartate ester) block copolymers (Yokoyama et al., 2004; Kawakami et al., 2005; Watanabe et al., 2006; Chansri et al., 2008). These observations prompted us to investigate the potential use of polymeric micelle formulations by optimizing the hydrophobic segments with esterified functional groups to enhance the blood retention of 4-HPR following intravenous administration. Here, four types of poly(ethylene glycol)-poly(aspartate ester) block copolymers with different esterified functional groups were synthesized to optimize the

* Corresponding author. Tel.: +81 75 753 4545; fax: +81 75 753 4575.
E-mail address: hashidam@pharm.kyoto-u.ac.jp (M. Hashida).

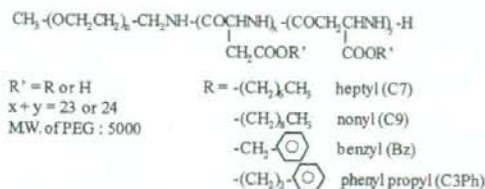


Fig. 1. Schematic illustration of synthesized block copolymers.

Poly(ethylene glycol)–poly(aspartate ester) block copolymers were obtained by an esterification reaction between a bromide compound and the aspartic acid residue of poly(ethylene glycol)–poly(aspartic acid) block copolymers (Yokoyama et al., 2004). Block copolymers with heptyl, nonyl, benzyl and phenyl propyl groups are abbreviated as C7, C9, Bz and C3Ph, respectively. The esterification level determined by ^1H NMR is expressed as a % value following the block copolymer abbreviation. 4-HPR encapsulated polymeric micelles were prepared by a conventional evaporation method modified as described in our previous report (Kawakami et al., 2005). The ratio of block copolymers/4-HPR for their preparation was fixed as 2.5 (weight ratio). As a control, poly(ethylene glycol) modified liposomes (PEG liposomes) were selected to evaluate the potentials of novel polymeric micelle formulations because of their wide use in cancer chemotherapy (Torchilin, 2005).

The physicochemical properties, such as the particle size and zeta potential of the macromolecules, are determining factors for their biodistribution (Takakura and Hashida, 1996). For escape

stable encapsulation of 4-HPR in the inner core of polymeric micelles (Fig. 1).

Since the *in vivo* drug release from particulate carriers is much higher than that from *in vitro* drug release (Takino et al., 1993; Shabbits et al., 2002), *in vivo* evaluation is important for the development of polymeric micelles for 4-HPR encapsulation. Therefore, the blood concentration of 4-HPR following intravenous administration of 4-HPR encapsulated polymeric micelles into the tail vein of mice was measured using HPLC.

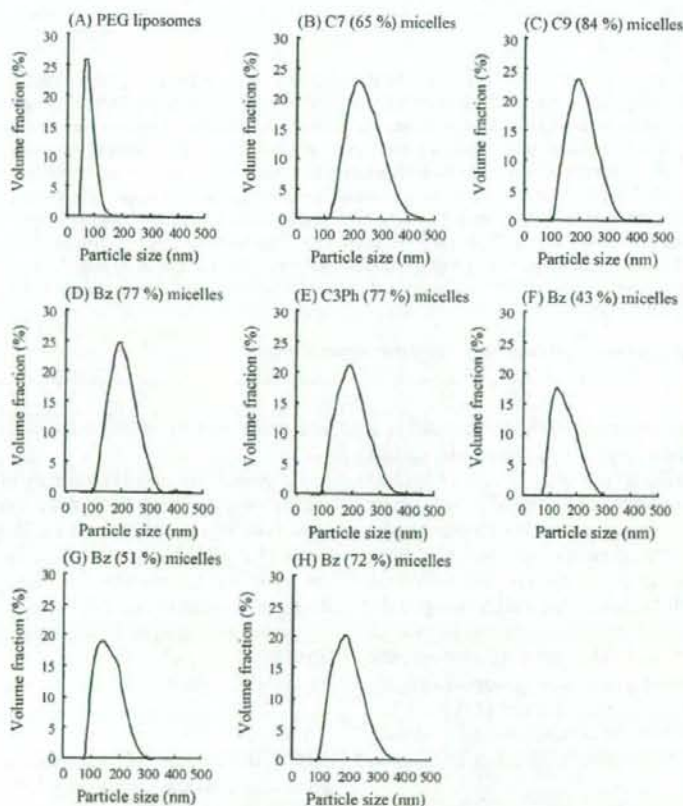


Fig. 2. Size distribution of 4-HPR encapsulated PEG liposomes (A) and polymeric micelles with several types and levels of esterified functional groups (B–H). 4-HPR encapsulated PEG liposomes were composed of hydrogenated soybean phosphatidyl choline (HSPC), cholesterol, distearoylphosphatidylethanolamine-*N*-[methoxy(polyethylene glycol)-2000] (PEG-DSPE), and 4-HPR (33.3:16.7:1.67:1, molar ratio). The ratio of block copolymers/4-HPR for 4-HPR encapsulated polymeric micelles was fixed as 2.5 (weight ratio). They were prepared by a conventional evaporation method modified as described in our previous report (Kawakami et al., 2005).

Table 1
Zeta potential of 4-HPR encapsulated PEG liposomes (A) and polymeric micelles with several types and levels of esterified functional groups (B-H)

Carrier	Zeta potential (mV)
(A) PEG liposomes	-2.7 ± 1.4
(B) C7 (65%) micelles	-1.7 ± 0.7
(C) C9 (84%) micelles	-2.6 ± 1.0
(D) Bz (77%) micelles	-1.4 ± 1.2
(E) C3Ph (77%) micelles	-0.8 ± 0.8
(F) Bz (43%) micelles	-10.7 ± 1.8
(G) Bz (51%) micelles	-3.1 ± 0.9
(H) Bz (72%) micelles	-2.3 ± 3.2

Each value represents the means ± S.D. (n=3-4).

of uptake by the reticuloendothelial system and long-term blood retention in the systemic circulation, it is needed that the particle size and zeta potential of PEG modified particulates (liposomes and polymeric micelles) are about <200 nm and weak anion (Oku and Namba, 1994; Nishiyama et al., 2003). Therefore, the mean particle size and zeta potential of 4-HPR encapsulated polymeric micelles were measured using Zetasizer Nano Series (Malven Instruments Ltd., Worcestershire, UK). As shown in Fig. 2 and Table 1, the mean particle size and zeta potential of all 4-HPR encapsulated polymeric micelles ranged from 142 to 225 nm and from -10.7 to -0.8 mV respectively, not dramatically changed irrespective of types and levels of esterified functional groups. The mean particle size and zeta potential of 4-HPR encapsulated PEG liposomes were about 76 nm and -2.7 mV. Thus, 4-HPR encapsulated polymeric micelles and PEG liposomes can avoid uptake by the reticuloendothelial system and enhance the blood retention of 4-HPR after intravenous administration.

After intravenous administration of 4-HPR itself (dissolved in polyoxyethylene hydrogenated castor oil (HCO-60), which was a solubilizing agent) and 4-HPR encapsulated PEG liposomes at 1 h, the blood concentration of 4-HPR was about 2.8% and 2.2% of the dose/mL (Fig. 3), suggesting the rapid release of 4-HPR from PEG liposomes. From the reports of Swanson et al. (1980) and Hultin et al. (1986), the blood concentration of 4-HPR at 1 h after intravenous injection was calculated to be about

3% of the dose/mL, supporting our result. In contrast, the blood concentration of 4-HPR was about 22-34% of the dose/mL after intravenous administration of 4-HPR encapsulated polymeric micelles, suggesting the stable encapsulation of 4-HPR by these types of polymeric micelles. Among them, the polymeric micelles prepared by block copolymers (Bz (77%)) exhibited the highest blood concentration of 4-HPR. Recently, Kataoka et al. reported that doxorubicin can be stably encapsulated in polymeric micelles prepared by poly(ethylene glycol)-poly(β -benzyl-L-aspartate) block copolymers through π - π stacking (Kataoka et al., 2000). Therefore, 4-HPR, which possesses a benzene ring, might be also stably encapsulated in polymeric micelles prepared by block copolymers (Bz (77%)) through this π - π stacking. As far as the effects of the level of Bz groups in the block copolymers are concerned, the blood concentration of 4-HPR was enhanced by Bz groups at a level of 72% and 77%, not by Bz groups at a level of 43% and 51% (Fig. 4). These results suggest that 4-HPR is stably encapsulated in polymeric micelles prepared by block copolymers (Bz) although a level of over 72% of Bz groups in block copolymers is needed.

Furthermore, long-term biodistribution of 4-HPR after intravenous injection of 4-HPR encapsulated polymeric micelles prepared by block copolymers (Bz (77%)) was evaluated. After intravenous injection of 4-HPR itself (dissolved in HCO-60), 4-HPR was rapidly eliminated from blood circulation and highly distributed in liver (Fig. 5). In addition, all of tissue to blood concentration ratio (K_p) of 4-HPR were increased as time passed, especially K_p value on kidney at 8 h was most high compared with other tissues (Fig. 6). These trends were supported by other report with different intravenous formulation of 4-HPR (Swanson et al., 1980). On the other hand, 4-HPR encapsulated polymeric micelles prepared by block copolymers (Bz (77%)) showed much higher blood concentration of 4-HPR for more than 8 h and lower liver distribution of 4-HPR until 1 h compared with 4-HPR itself (Fig. 5). These results indicated that, 4-HPR encapsulated polymeric micelles prepared by block copolymers (Bz (77%)) showed prolonged circulation of 4-HPR for stable encapsulation of 4-HPR and escape of initial uptake by liver. The mean area under the curve (AUC_{0-8h}) in blood of 4-HPR itself

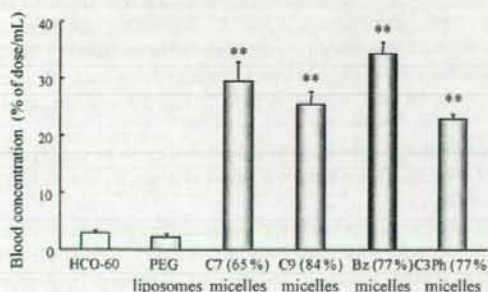


Fig. 3. Blood concentration of 4-HPR itself (dissolved in HCO-60), 4-HPR encapsulated in PEG liposomes, and in polymeric micelles with several types of esterified functional groups at 1 h after intravenous injection into mice at a dose of 5 mg/kg as 4-HPR. Each value represents the means ± S.D. (n=3-4). **P<0.01, compared with HCO-60 groups.

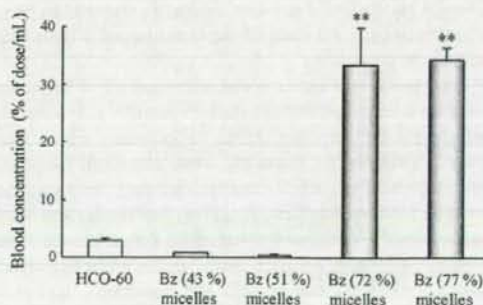


Fig. 4. Effect of level of Bz groups in block copolymers on blood concentration of 4-HPR encapsulated in Bz micelles at 1 h after intravenous injection into mice at a dose of 5 mg/kg as 4-HPR. Each value represents the means ± S.D. (n=3-4). **P<0.01, compared with HCO-60 groups.

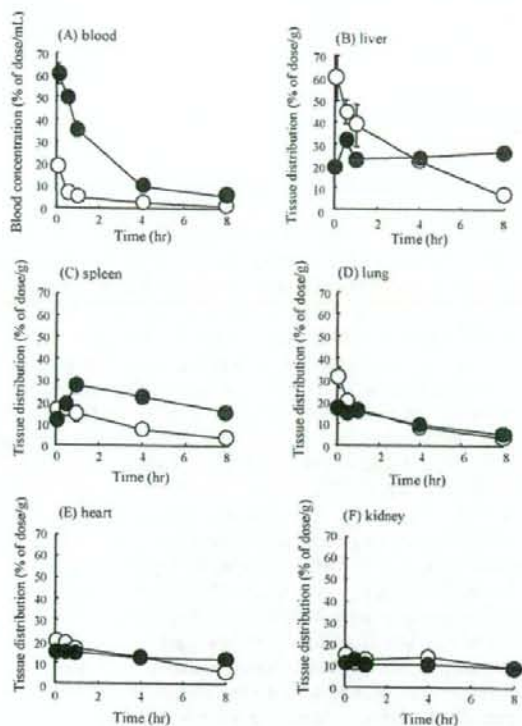


Fig. 5. Blood concentration (A) or tissue accumulation (liver (B), spleen (C), lung (D), heart (E), kidney (F)) of 4-HPR itself (dissolved in HCO-60) (○) and 4-HPR encapsulated in Bz (77%) micelles (●) after intravenous injection into mice at a dose of 5 mg/kg as 4-HPR. Each value represents the mean \pm S.D. ($n = 3-4$).

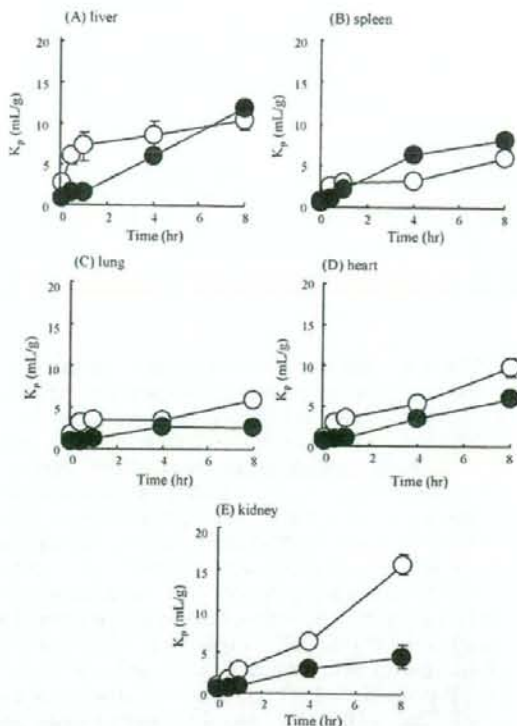


Fig. 6. Tissue to blood concentration ratio (K_p) of 4-HPR in liver (A), spleen (B), lung (C), heart (D), and kidney (E) of 4-HPR itself (dissolved in HCO-60) (○) and 4-HPR encapsulated in Bz (77%) micelles (●) after intravenous injection into mice at a dose of 5 mg/kg as 4-HPR. Each value represents the mean \pm S.D. ($n = 3-4$).

and 4-HPR encapsulated in Bz (77%) micelles calculated by the linear trapezoidal rule was 26.4 and 148 (% of dose \times h/mL) and its relative AUC ratio was 5.6. Furthermore, K_p in lung, heart, and kidney after intravenous injection of 4-HPR encapsulated polymeric micelles prepared by block copolymers (Bz (77%)) were lower than that of 4-HPR itself (Fig. 6), suggesting that 4-HPR encapsulated polymeric micelles prepared by block copolymers (Bz (77%)) escaped the transition of 4-HPR from blood to these tissues.

In this study, enhanced blood retention of 4-HPR was achieved by using polymeric micelles prepared by poly(ethylene glycol)-poly(aspartate ester) block copolymers, which were optimized hydrophobic segments with esterified functional groups. In particular, 4-HPR encapsulated polymeric micelles prepared by block copolymers (Bz (77%)) had the highest blood concentration of 4-HPR, which was about 106 μ M (34% of the dose/mL) at a dose of 5 mg/kg. As far as the pharmacological effects of 4-HPR on cancer cells are concerned, Kalemkerian et al. have reported that 4-HPR efficiently inhibited the growth of small-cell lung cancer cell line and its IC_{50} values ranged from 0.1 to 3.0 μ M (Kalemkerian et al., 1995). The neo-vascularization formed by solid tumors exhibits some unique

features, such as hypervascularity, leaky capillaries and poor lymphatic clearance. These characteristics cause the accumulation of macromolecules in tumors for a long period, known as enhanced permeability and retention (EPR) effects (Matsumura and Maeda, 1986). The spaces in the blood endothelium formed by solid tumors are reported to range from 300 to 4700 nm (Yuan et al., 1995; Hashizume et al., 2000). Since the mean diameter of 4-HPR encapsulated polymeric micelles prepared by block copolymers (Bz (77%)) is about 175 nm, and maximally 342 nm, these may be small enough to pass through the endothelium of solid tumors. These observations led us to believe that 4-HPR encapsulated polymeric micelles prepared by block copolymers (Bz (77%)) could be effective carrier systems for use in future cancer therapy.

In conclusion, poly(ethylene glycol)-poly(aspartate ester) block copolymers with heptyl, nonyl, benzyl and phenyl propyl groups (abbreviated as C7, C9, Bz and C3Ph) were synthesized for stable encapsulation of 4-HPR. It is suggested that 4-HPR is stably encapsulated in polymeric micelles prepared by block copolymers (Bz) although a level of over 72% of Bz groups in the block copolymers is needed for stable encapsulation of 4-HPR. The information we have obtained in this study will be of

value for the future use, design, and development of polymeric micelles involving the *in vivo* application of 4-HPR.

Acknowledgements

This work was supported in part by Grants-in-Aid for Scientific Research and the Program for Promoting the Establishment of Strategic Research Centers, Special Coordination Funds for Promoting Science and Technology from the Ministry of Education, Culture, Sports, Science, and Technology of Japan, and by the Health and Labour Sciences Research Grants for Research on Advanced Medical Technology from the Ministry of Health, Labour and Welfare of Japan. Yokoyama M. and Yamamoto T. acknowledge support by the Program for Promoting the Establishment of Strategic Research Centers, Special Coordination Funds for Promoting Science and Technology from the Ministry of Education, Culture, Sports, Science, and Technology of Japan.

References

Chansri, N., Kawakami, S., Yokoyama, M., Yamamoto, T., Charoensit, P., Hashida, M., 2008. Anti-tumor effect of all-trans retinoic acid loaded polymeric micelles in solid tumor bearing mice. *Pharm. Res.* 25, 428–434.

Formelli, F., Clerici, M., Campa, T., Di Mauro, M.G., Magni, A., Mascotti, G., Moglia, D., De Palo, G., Costa, A., Veronesi, U., 1993. Five-year administration of fenretinide: pharmacokinetics and effects on plasma retinol concentrations. *J. Clin. Oncol.* 11, 2036–2042.

Formelli, F., Barua, A.B., Olson, J.A., 1996. Bioactivities of *N*-(4-hydroxyphenyl) retinamide and retinoyl beta-glucuronide. *FASEB J.* 10, 1014–1024.

Gaucher, G., Dufresne, M.H., Sant, V.P., Kang, N., Maysinger, D., Leroux, J.C., 2005. Block copolymer micelles: preparation, characterization and application in drug delivery. *J. Control Release* 109, 169–188.

Hashizume, H., Baluk, P., Morikawa, S., McLean, J.W., Thurston, G., Roberge, S., Jain, R.K., McDonald, D.M., 2000. Openings between defective endothelial cells explain tumor vessel leakiness. *Am. J. Pathol.* 156, 1363–1380.

Hultin, T.A., May, C.M., Moon, R.C., 1986. *N*-(4-Hydroxyphenyl)-all-trans-retinamide pharmacokinetics in female rats and mice. *Drug Metab. Dispos.* 14, 714–717.

Kalemkerian, G.P., Slusher, R., Ramalingam, S., Gadgeel, S., Mabry, M., 1995. Growth inhibition and induction of apoptosis by fenretinide in small-cell lung cancer cell lines. *J. Natl. Cancer Inst.* 87, 1674–1680.

Kataoka, K., Matsumoto, T., Yokoyama, M., Okano, T., Sakurai, Y., Fukushima, S., Okamoto, K., Kwon, G.S., 2000. Doxorubicin-loaded poly(ethylene glycol)-poly(beta-benzyl-L-aspartate) copolymer micelles: their pharmaceutical characteristics and biological significance. *J. Control Release* 64, 143–153.

Kataoka, K., Harada, A., Nagasaki, Y., 2001. Block copolymer micelles for drug delivery: design, characterization and biological significance. *Adv. Drug Deliv. Rev.* 47, 113–131.

Kawakami, S., Opanasopit, P., Yokoyama, M., Chansri, N., Yamamoto, T., Okano, T., Yamashita, F., Hashida, M., 2005. Biodistribution characteristics of all-trans retinoic acid incorporated in liposomes and polymeric micelles following intravenous administration. *J. Pharm. Sci.* 94, 2606–2615.

Kokate, A., Li, X., Jasti, B., 2006. Transport of a novel anti-cancer agent, fenretinide across Caco-2 monolayers. *Invest. New Drugs* 25, 197–203.

Matsumura, Y., Maeda, H., 1986. A new concept for macromolecular therapeutics in cancer chemotherapy: mechanism of tumorotropic accumulation of proteins and the antitumor agent smancs. *Cancer Res.* 46, 6387–6392.

Nishiyama, N., Okazaki, S., Cabral, H., Miyamoto, M., Kato, Y., Sugiyama, Y., Nishio, K., Matsumura, Y., Kataoka, K., 2003. Novel cisplatin-incorporated polymeric micelles can eradicate solid tumors in mice. *Cancer Res.* 63, 8977–8983.

Oku, N., Namba, Y., 1994. Long-circulating liposomes. *Crit. Rev. Ther. Drug Carrier Syst.* 11, 231–270.

Raffaghello, L., Pagnan, G., Pastorino, F., Cosimo, E., Brignole, C., Marimpietri, D., Montaldo, P.G., Gambini, C., Allen, T.M., Bogenmann, E., Fonzoni, M., 2003. In vitro and in vivo antitumor activity of liposomal Fenretinide targeted to human neuroblastoma. *Int. J. Cancer* 104, 559–567.

Shabbits, J.A., Chiu, G.N., Mayer, L.D., 2002. Development of an in vitro drug release assay that accurately predicts in vivo drug retention for liposome-based delivery systems. *J. Control Release* 84, 161–170.

Swanson, B.N., Zaharevitz, D.W., Sporn, M.B., 1980. Pharmacokinetics of *N*-(4-hydroxyphenyl)-all-trans-retinamide in rats. *Drug Metab. Dispos.* 8, 168–172.

Takahashi, N., Tamagawa, K., Shimizu, K., Fukui, T., Maitani, Y., 2003. Effects on M5076-hepatic metastasis of retinoic acid and *N*-(4-hydroxyphenyl) retinamide, fenretinide entrapped in SG-liposomes. *Biol. Pharm. Bull.* 26, 1060–1063.

Takakura, Y., Hashida, M., 1996. Macromolecular carrier systems for targeted drug delivery: pharmacokinetic considerations on biodistribution. *Pharm. Res.* 6, 820–831.

Takino, T., Nakajima, C., Takakura, Y., Sezaki, H., Hashida, M., 1993. Controlled biodistribution of highly lipophilic drugs with various parenteral formulations. *J. Drug Target J.* 1, 117–124.

Torchilin, V.P., 2005. Recent advances with liposomes as pharmaceutical carriers. *Nat. Rev. Drug Discov.* 4, 145–160.

Watanabe, M., Kawano, K., Yokoyama, M., Opanasopit, P., Okano, T., Maitani, Y., 2006. Preparation of camptothecin-loaded polymeric micelles and evaluation of their incorporation and circulation stability. *Int. J. Pharm.* 308, 183–189.

Yokoyama, M., Opanasopit, P., Okano, T., Kawano, K., Maitani, Y., 2004. Polymer design and incorporation methods for polymeric micelle carrier system containing water-insoluble anti-cancer agent camptothecin. *J. Drug Target* 12, 373–384.

Yuan, F., Dellian, M., Fukumura, D., Leunig, M., Berk, D.A., Torchilin, V.P., Jain, R.K., 1995. Vascular permeability in a human tumor xenograft: molecular size dependence and cutoff size. *Cancer Res.* 55, 3752–3756.



Colloids and Surfaces B: Biointerfaces

journal homepage: www.elsevier.com/locate/colsurfb

A simple hemostasis model for the quantitative evaluation of hydrogel-based local hemostatic biomaterials on tissue surface

Yoshihiko Murakami^{a,*}, Masayuki Yokoyama^{b,*}, Hiroshi Nishida^c, Yasuko Tomizawa^c, Hiromi Kurosawa^c^a Department of Organic and Polymer Materials Chemistry, Faculty of Engineering, Tokyo University of Agriculture and Technology, Tokyo 184-8588, Japan^b Yokoyama Nano-Medical Polymers Project, Kanagawa Academy of Science and Technology (KAST), Kanagawa, Japan^c Department of Cardiovascular Surgery, The Heart Institute of Japan, Tokyo Women's Medical University, Tokyo, Japan

ARTICLE INFO

Article history:

Received 18 March 2008

Received in revised form 30 March 2008

Accepted 7 April 2008

Available online 18 April 2008

Keywords:

Hemostatic hydrogel

Surgical sealant

Quantitative evaluation

Tissue surface

Biointerface

ABSTRACT

Several hemostat hydrogels are clinically used, and some other agents are studied for safer, more facile, and more efficient hemostasis. In the present paper, we proposed a novel method to evaluate local hemostat hydrogel on tissue surface. The procedure consisted of the following steps: (step 1) a mouse was fixed on a cork board, and its abdomen was incised; (step 2) serous fluid was carefully removed because it affected the estimation of the weight gained by the filter paper, and parafilm and preweighted filter paper were placed beneath the liver (parafilm prevented the filter paper's absorption of gradually oozing serous fluid); (step 3) the cork board was tilted and maintained at an angle of about 45° so that the bleeding would more easily flow from the liver toward the filter paper; and (step 4) the bleeding lasted for 3 min. In this step, a hemostat was applied to the liver wound immediately after the liver was pricked with a needle. We found that (1) a careful removal of serous fluid prior to a bleeding and (2) a quantitative determination of the amount of excess aqueous solution that oozed out from a hemostat were important to a rigorous evaluation of hemostat efficacy. We successfully evaluated the efficacy of a fibrin-based hemostat hydrogel by using our method. The method proposed in the present study enabled the quantitative, accurate, and easy evaluation of the efficacy of local hemostatic hydrogel which acts as tissue-adhesive agent on biointerfaces.

© 2008 Elsevier B.V. All rights reserved.

1. Introduction

Local hemostatic hydrogels are applied to surgical wounds in order to arrest bleeding from both suture holes and cross-sectional surfaces of parenchymatous organs in cases wherein the use of cautery, ligature, or other conventional hemostatic methods is impractical. The local hemostatic agents include fibrin glue, gelatin-sponge/powder, collagen-sponge/powder/fiber/sheet, oxidized cellulose, and collagen- or gelatin-based hemostatic agents [1]. Moreover, tissue adhesives (such as (1) gelatin with resorcin and formalin, (2) albumin with glutaraldehyde, (3) cyanoacrylate, and (4) synthetic polymers) used for stopping serous fluid and air leaks are also studied for hemostasis [2,3]. Fibrin glues have been widely used in a variety of surgical procedures and are designed to mimic the physiology of the final steps of the blood coagulation

cascade. However, there is a risk of infectious contaminations. Collagen and gelatin have high tensile strength, absorbability in the body, and good cell compatibility. They are, however, not suitable as tissue-contacting materials owing to the same risk factor (infectious contaminations). Since synthetic glues do not possess the risk of infectious contaminations, the glues have been actively developed in recent years. For example, cyanoacrylate polymer is comparable to fibrin glues, but it offers additional benefits such as a relatively high bonding strength and no risk of infectious contaminations.

It is important to establish an easy method for the quantitative determination of the efficacy of local hemostatic agents. Various methods have been proposed for the evaluation of hemostat efficacy. For example, Chvapil et al. established a method by which they could arrest moderate bleeding from an anesthetized dog's spleen (bleeding that was induced with a 0.5-cm deep and 4-cm-wide wedge excision) [4]. By means of this method, it was clarified that a hemostatic agent with a sheet-like structure and a hemostatic agent with collagen could stop the bleeding within 3 min, whereas gelatin-sponge or oxidized cellulose materials were less effective. Prior et al. proposed a method wherein estimates of total bleeding

* Corresponding author. Tel.: +81 42 388 7387; fax: +81 42 388 7387.

** Corresponding author. Tel.: +81 44 819 2093; fax: +81 44 819 2095.

E-mail addresses: ymuraki@nodai.ac.jp (Y. Murakami),yokoyama@ksc.kanagawa.ac.jp (M. Yokoyama).

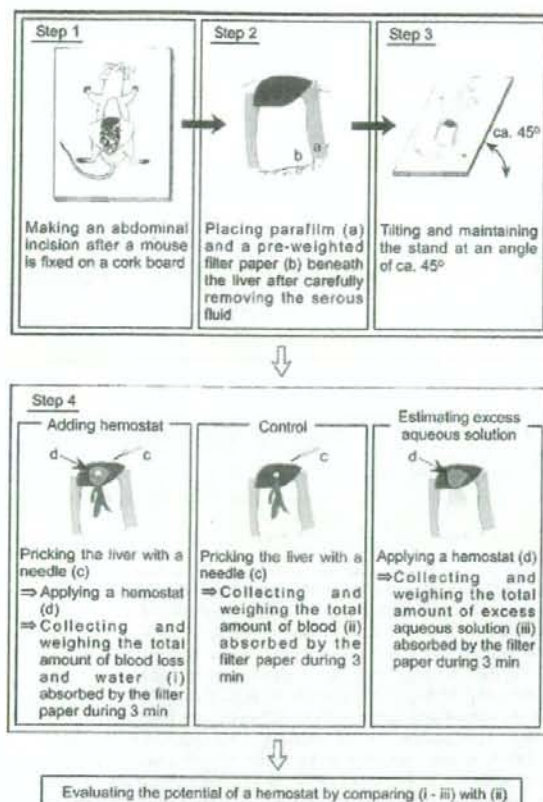


Fig. 1. The proposed method, based on a mouse-hemostasis model, for the quantitative evaluation of local-hemostat hydrogel efficacy on tissue surface.

derived from the weight gained by the preweighted gauze squares or cotton swabs was used to absorb uncoagulated blood from the surgical field of a rabbit kidney [5].

None of these methods are, however, satisfactory for the quantitative determination of the efficacy of local hemostatic agents, because they (1) do not simulate the actual situation where local hemostatic agents are clinically used (i.e., although the rapid completion of a local hemostasis is critical to surgery, some reports neglect how important it is to reduce the formation time of hemostats) or (2) do not present quantitative evaluations, or (3) necessitates complicated procedures. In the present paper, we proposed a novel method to evaluate the efficacy of local hemostat hydrogel on tissue surface.

2. Materials and methods

Fig. 1 illustrates the procedure of the proposed method. The method consists of the following steps: (step 1) a mouse is fixed on a surgical cork board and an abdominal incision was made; (step 2) serous fluid is carefully removed because it affects the estimation of the weight gained by the filter paper, and parafilm and filter paper preweighted by a balance are placed beneath the liver (parafilm prevents the filter paper's absorption of gradually oozing serous fluid); (step 3) the cork board is tilted and maintained at an angle of about 45° to assist the flow of the bleeding from the liver toward the filter paper; and (step 4) the bleeding lasts for 3 min. In this step, a hemostatic agent that is to be evaluated is applied to the

liver wound immediately after the liver is pricked with a needle. Also, we performed control experiments (wherein a hemostat is not applied after the liver is pricked with a needle). The operator was blinded so that he did not know whether or not a hemostat was applied in each run (a blind test). The sterile needle (18G, 38 mm, Terumo Corp., Japan) was used for the pricking of the liver. Control experiments were also done, in which we applied a hemostat to the unpricked liver in order to measure the amount of the excess aqueous solution that the filter paper absorbed. This experiment was important because the excess solution oozed out from the hemostat hydrogel during its formation. If this excess solution is not carefully determined and subtracted from the total amount of weight gained in the filter paper, the measured blood would be unjustly higher than the actual amount of blood through bleeding. We determined both the amount of the blood loss and the aqueous solutions after removing the hemostat hydrogel from the filter paper. Cases in which excessive bleeding (blood from the liver reached to the filter paper beneath the liver within 2 s) was seen due to ripping of the liver rather than pricking of the liver were excluded from the evaluation.

We used a fibrin-based hemostat Tisseel™ hydrogel (Baxter, IL) to assess the proposed method. We used 15 ddY mice to evaluate the hemostatic potential of Tisseel, and three ddY mice to estimate the amount of excess solution that oozed out during the hemostat formation. The average weight of the mice was 24.3 g (S.D. 0.61 g). Prior to an abdominal incision, the mice received an intraperitoneal injection of pentobarbital sodium (Nembutal™, Dainippon Pharmaceutical Co. Ltd., Japan). We mixed an aprotinin solution containing fibrinogen and a calcium chloride solution containing thrombin to form a hemostat gel with a dual-chamber applicator. All experiments are performed at room temperature. We performed a statistical analysis of the data by using the two-sided Student's *t*-test. A *P*-value < 0.05 indicated statistical significance.

All animal experiments were carried out according to the Principle of Laboratory Animal Care, the Guide for the Care and Use of Laboratory Animals, and guidelines of the animal care committee in our institute (Tokyo Women's Medical University).

3. Results and discussion

Hydrogel-based adhesives are used for tissue adhesion, hemostasis, and sealing of the leakage of air and body fluids during surgical procedures. The quantitative determination of the efficacy of local hemostatic agents is difficult, because they do not simulate the actual situation where local hemostatic agents are clinically used, do not present quantitative evaluations, and necessitates complicated procedures. In the present paper, we tried to propose a novel method to evaluate local hemostat hydrogel on tissue surface. The procedure consisted of the following easy steps: (1) the fixing of a mouse; (2) the careful removal of serous fluid; (3) the tilting of the cork board at an angle of about 45°; and (4) the bleeding test. The method proposed in the present article can be applied to any surgical site. However, liver was used as a surgical site in a novel mouse model because liver was easy to be exposed.

Fig. 2 shows typical photographs for the Tisseel applications. Tisseel consists of a two-component fibrin matrix that offers highly concentrated human fibrinogen to seal tissue and stop diffuse bleeding. The mixture of the Tisseel gel and the coagulated blood formed after Tisseel was applied to the wound, and consequently, a bleeding was arrested. Tisseel has been used as an adjunct to hemostasis in surgeries involving cardiopulmonary bypass and treatment of splenic injuries due to blunt or penetrating trauma to the abdomen, when control of bleeding by conventional surgical

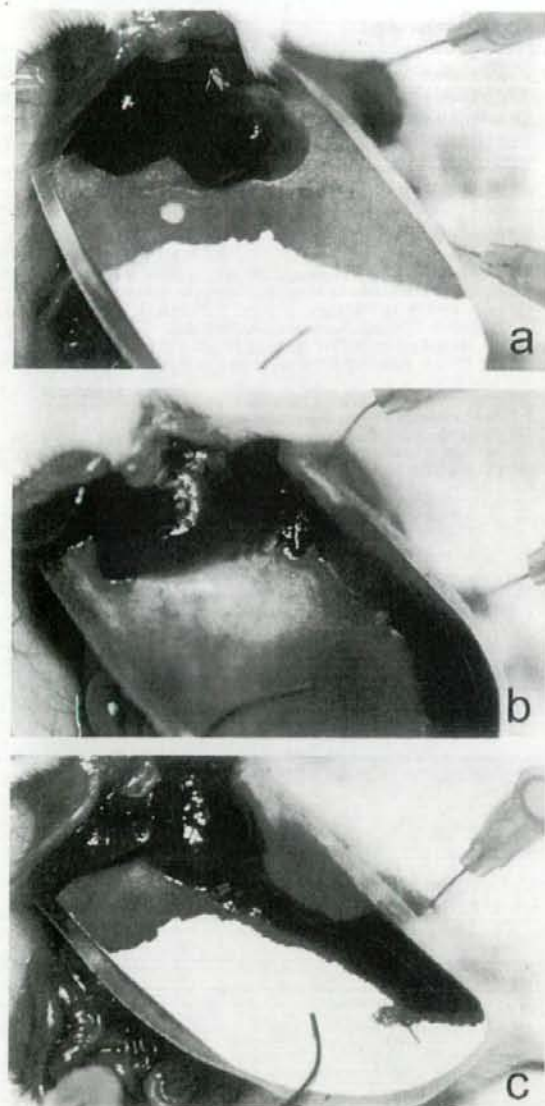


Fig. 2. The typical photographs of Tisseel applications (a: entry 9; b: entry 7; c: entry 8).

techniques, including suture, ligature and cautery, is ineffective or impractical.

Two phenomena were observed in the Tisseel applications. First, the mixture weakly adhered to the tissue surface and arrested the liver hemorrhage (Fig. 2(a)) and second, the mixture did not adhere to the tissue surface and moved slightly owing to bloodstream's force (Fig. 2(b)). The difference between these two phenomena presumably depended on the difference between the rate at which the gel formed and the rate at which the Tisseel gel adhered to the tissue surface. If the gel formation occurred before the gel adhesion, the gel could not successfully anchor to the tissue's uneven surface, resulting in poor tissue adhesiveness. The two phenomena show that Tisseel has poor tissue adhesiveness in such a case as that shown in Fig. 2(b). This observation is the same as that previously

Table 1
Evaluation of the amount of bleeding with (+) or without (–) Tisseel applications (in entries 7 and 8, two filter papers were used)

Entry	Tisseel	Filter paper (mg)	Filter paper + blood (mg)	Blood (mg)
1	+	104	226	122
2	–	107	222	115
3	+	107	283	176
4	+	104	313	209
5	–	103	301	198
6	–	106	249	143
7	+	106	395	289 (289+22)
		100	122	
8	–	105	382	277 (277+105)
		101	249	
9	+	103	205	102
10	–	107	178	71
11	+	101	248	147
12	–	103	259	156
13	+	105	276	171
14	+	103	311	208
15	–	104	147	43

reported for another fibrin-based glue, BOLHEAL™ [6], where the poly(L-glutamic acid)-based glue exhibited good adhesiveness to tissues where BOLHEAL readily detached. The easy detachment was also clinically observable. In contrast, bleeding was not arrested in the control experiment (Fig. 2(c)).

We found that careful removal of serous fluid prior to bleeding and quantification of the amount of excess aqueous solution that oozed out from a hemostat were important to a rigorous quantitative evaluation of hemostats efficacy. Table 1 summarizes results of the Tisseel applications. The bleeding from the mouse liver was affected by a number of factors such as blood pressure of the mouse and size of the mouse liver. Since these factors were difficult to be controlled in animal experiments, we consider that the difference in bleeding (which is listed in Table 1) was within experimental error. We used 15 mice to minimize the effect of the experimental error.

The average bleeding was 145.9 mg (S.D. 115.6 mg, $N=7$) in the control experiments, whereas it was 180.8 mg (S.D. 64.8 mg, $N=8$) when Tisseel was applied to the wound ($P=0.50$). Although Tisseel exhibited a hemostatic potential, the P -value was unexpectedly high; this was because the amount of excess solution was not considered in the evaluation. The excess solution oozed out from Tisseel after the two precursor solutions were mixed with each other. The average amount of excess solution was 137.0 mg (S.D. 38.5 mg, $N=3$). After a subtraction of the excess solution amount, the reevaluated average bleeding was only 43.8 mg (S.D. 64.8 mg, $N=7$) in mice to whose wounds Tisseel was applied. This value showed that Tisseel had a relatively significant hemostatic potential ($P=0.07$). The difference between the two P values (0.50 and 0.07) showed how important it is to consider the excess solution for the hemostasis evaluations. It is noteworthy that the subtraction of the excess-solution amount from the total measured bleeding has not been considered in previously reported animal hemostasis models [4,5].

Thus, we concluded that the method proposed in the present study facilitated a quantitative, accurate, and easy evaluation of the efficacy of local hemostat hydrogels on tissue surface.

4. Conclusions

Several hemostat hydrogels have been studied for safer, more facile, and more efficient hemostasis. In the present paper, we proposed a novel method to evaluate local hemostat hydrogel on tissue surface. We found that (1) a careful removal of

serous fluid prior to a bleeding and (2) a quantitative determination of the amount of excess aqueous solution that oozed out from a hemostat were important to a rigorous evaluation of hemostat efficacy. We successfully evaluated the efficacy of a fibrin-based hemostat hydrogel by using our method. Hydrogels, which are three-dimensional cross-linked polymer networks that swell, but are insoluble in water, have various functional properties, such as the ability to absorb a significant amount of water and flexibility similar to a natural tissue. These properties have provided many potential applications particularly in biotechnological and medical fields [7–10]. The evaluation of the hydrogel properties on biointerfaces is needed subject for the development of better materials. The method proposed in the present study enabled the quantitative, accurate, and easy evaluation of the efficacy of local hemostatic hydrogel which acts as tissue-adhesive agent on biointerfaces. Although further work concerning the generalization of the method proposed in the present study is required, the results obtained indicate that the novel methods can be used for quantitative evaluation of the efficacy of surgical biomaterials.

Acknowledgements

This study was funded, in part, by Grants-in-Aid for Scientific Research (Grant-in-Aid for Young Scientists B and Exploratory Research) from the Ministry of Education, Culture, Sports, Science and Technology of Japan (MEXT) and the Industrial Technology Research Grant Program from New Energy and Industrial Technology Development Organization (NEDO) of Japan.

References

- [1] Y. Tomizawa, *J. Artif. Organs* 8 (2005) 137.
- [2] T.B. Reece, T.S. Maxey, L.L. Kron, *Am. J. Surg.* 182 (2001) 405.
- [3] Y. Murakami, M. Yokoyama, T. Okano, H. Nishida, Y. Tomizawa, M. Endo, H. Kurosawa, *J. Biomed. Mater. Res.* 80A (2007) 421.
- [4] M. Chvapil, J.A. Owen, D.W. DeYoung, *J. Trauma* 23 (1983) 1042.
- [5] J.J. Prior, N. Powers, F. DeLustro, *J. Biomed. Mater. Res. (Appl. Biomater.)* 53 (2000) 252.
- [6] Y. Otani, Y. Tabata, Y. Ikada, *J. Biomed. Mater. Res.* 31 (1996) 157.
- [7] Y. Murakami, M. Maeda, *Macromolecules* 38 (2005) 1535.
- [8] Y. Murakami, M. Maeda, *Biomacromolecules* 6 (2005) 2927.
- [9] H.J. van der Linden, S. Herber, W. Olthuis, P. Bergveld, *Analyst* 128 (2003) 325.
- [10] Y. Qui, K. Park, *Adv. Drug Deliv. Rev.* 53 (2001) 321.



Note

Particle size-dependent triggering of accelerated blood clearance phenomenon

Hiroyuki Koide^a, Tomohiro Asai^a, Kentaro Hatanaka^a, Takeo Urakami^a, Takayuki Ishii^a,
Eriya Kenjo^a, Masamichi Nishihara^b, Masayuki Yokoyama^b, Tatsuhiro Ishida^c,
Hiroshi Kiwada^c, Naoto Oku^{a,*}

^a Department of Medical Biochemistry and Global COE Program, Graduate School of Pharmaceutical Sciences, University of Shizuoka, 52-1 Yada, Suruga-ku, Shizuoka 422-8526, Japan

^b Kanagawa Academy of Science and Technology, KSP East 404, Sakado 3-2-1, Takatsu-ku, Kawasaki, Kanagawa 213-0012, Japan

^c Department of Pharmacokinetics and Biopharmaceutics, Institute of Health Biosciences, The University of Tokushima, 1-78-1 Sho-machi, Tokushima 770-8505, Japan

ARTICLE INFO

Article history:

Received 22 April 2008

Received in revised form 29 May 2008

Accepted 4 June 2008

Available online 7 June 2008

Keywords:

Polyethylene glycol

Liposomes

Accelerated blood clearance

Polymeric micelles

Nanocarriers

ABSTRACT

A repeat-injection of polyethylene glycol-modified liposomes (PEGylated liposomes) causes a rapid clearance of them from the blood circulation in certain cases that is referred to as the accelerated blood clearance (ABC) phenomenon. In the present study, we examined whether polymeric micelles trigger ABC phenomenon or not. As a preconditioning treatment, polymeric micelles (9.7, 31.5, or 50.2 nm in diameter) or PEGylated liposomes (119, 261 or 795 nm) were preadministered into BALB/c mice. Three days after the preadministration [³H]-labeled PEGylated liposomes (127 nm) as a test dose were administered into the mice to determine the biodistribution of PEGylated liposomes. At 24 h after the test dose was given, accelerated clearance of PEGylated liposomes from the bloodstream and significant accumulation in the liver was observed in the mice preadministered with 50.2–795 nm nanoassemblies (PEGylated liposomes or polymeric micelles). In contrast, such phenomenon was not observed with 9.7–31.5 nm polymeric micelles. The enhanced blood clearance and hepatic uptake of the test dose (ABC phenomenon) were related to the size of triggering nanoassemblies. Our study provides important information for developing both drug and gene delivery systems by means of nanocarriers.

© 2008 Elsevier B.V. All rights reserved.

1. Introduction

PEGylated liposomes possessing a long-circulating characteristic have been widely used for delivery systems of both drugs and genes. PEG provides a steric barrier to nanocarriers for avoiding interaction with plasma proteins including opsonins and the cells of mononuclear phagocyte system (MPS) (Allen and Hansen, 1991; Sakakibara et al., 1996; Lasic, 1996). However, our recent reports demonstrated that the intravenous injection of PEGylated liposomes might significantly alter a pharmacokinetic behavior of them injected thereafter (Ishida et al., 2006a,c; Wang et al., 2007). A

repeat-injection of PEGylated liposomes causes a rapid clearance of them from the blood circulation in certain cases. This phenomenon, referred to as the accelerated blood clearance (ABC) phenomenon, is considered to be related with anti-PEG IgM secretion from splenic B cells (Ishida et al., 2006a,c). Anti-PEG IgM, produced in response to an injected dose of PEGylated liposomes, selectively binds to them injected secondary (Wang et al., 2007).

However, the immune response against polymeric micelles was not known at all. Polymeric micelles are formed from block copolymers typically consisting of hydrophilic and hydrophobic polymer blocks (Kwon and Kataoka, 1995). They are of particular interest as a drug carrier because of their small particle sizes, efficiency in entrapping a satisfactory amount of hydrophobic drugs within the inner core, stability in the circulation, and their ability of sustained release of the drugs. Polymeric micelles were also considered as a less immune response carrier (Yokoyama et al., 1991; Gaucher et al., 2005).

In this study, we examined whether the preadministration of polymeric micelles possessing PEG chains alters the biodistribution of PEGylated liposomes or not. Moreover, we investigated the

Abbreviations: ABC phenomenon, accelerated blood clearance phenomenon; [³H]-CHE, [³H] cholesterylhexadecyl ether; MPEGS-DSPE, 1,2-distearoyl-sn-glycero-3-phosphoethanolamine-n-[methoxy(polyethylene glycol)-2000]; MPS, mononuclear phagocyte system; PEG-PBLA, poly(ethylene glycol)-b-poly(β -benzyl L-aspartate); PEGylated liposomes, polyethylene glycol-modified liposomes.

* Corresponding author. Tel.: +81 54 264 5701; fax: +81 54 264 5705.

E-mail address: oku@u-shizuoka-ken.ac.jp (N. Oku).

particle size-dependency for triggering the phenomenon by use of PEGylated liposomes and polymeric micelles.

2. Materials and methods

2.1. Materials

Dipalmitoylphosphatidylcholine (DPPC), cholesterol and 1,2-distearoyl-*sn*-glycero-3-phosphoethanolamine-*n*-[methoxy(polyethylene glycol)-2000](MPEG-DSPE) were kindly gifted from Nippon Fine Chemical Co., Ltd. (Takasago, Hyogo, Japan). [³H]cholesterylhexadecyl ether ([³H]-CHE) was purchased from Amersham Pharmacia (Buckinghamshire, UK). All other reagents were analytical grade.

2.2. Animal

Five-week-old male BALB/c mice were purchased from Japan SLC Inc. (Shizuoka, Japan). The animals were cared for according to the animal facility guidelines of the University of Shizuoka. All animal experiments were approved by the Animal and Ethics Review Committee of the University of Shizuoka.

2.3. Preparation of polymeric micelles

Three block copolymers were used for polymeric micelle preparations. Their structures and compositions are summarized in Table 1. Poly(ethylene glycol)-*b*-poly(β -benzyl L-aspartate) (PEG-PBLA) was synthesized by polymerization of β -benzyl L-aspartate *N*-carboxy anhydride from an amino terminal of α -methyl- ω -aminopoly(oxyethylene), as reported previously (Yokoyama et al., 1992). Two partially esterified block copolymers, PEG-P(Asp(pentyl)) and PEG-P(Asp(nonyl)), were prepared by esterification of PEG-*b*-poly(aspartic acid) block copolymer by a reported method (Yamamoto et al., 2007). In brief, aspartic acid residues of PEG-*b*-poly(aspartic acid) block copolymer was activated with 1,8-diazabicyclo[5.4.0]undecene, followed by reaction with corresponding alkyl bromides, pentyl bromide and nonyl bromide.

Polymeric micelles were prepared from these three block copolymers by a dialysis method (Yamamoto et al., 2007). Block copolymers were dissolved in DMF at a concentration of 7.5 mg/ml. These polymer solutions were dialyzed against distilled water by the use of a dialysis membrane (Spectra/Por 6, molecular weight cut-off: 1000, Spectrum Japan, Tokyo, Japan). After overnight dialysis, the micelle solutions were concentrated by ultrafiltration (Millipore ultrafiltration membrane PBHK, molecular weight cut-off: 100,000, Nihon Millipore, Tokyo, Japan). By dynamic light scattering, weight-averaged diameters of the obtained polymeric micelles were found to be 50.2, 31.5, and 9.7 nm for PEG-PBLA, PEG-P(Asp(pentyl)), and PEG-P(Asp(nonyl)), respectively.

2.4. Preparation of PEGylated liposomes

PEGylated liposomes composed of DPPC and cholesterol with MPEG-DSPE (10:5:1 as molar ratio) were prepared as described previously (Maeda et al., 2004). In brief, lipids dissolved in chloroform were evaporated to form thin lipid film. Then liposomes were formed by hydration with 10 mM phosphate-buffered 0.3 M sucrose solution (pH 7.4). Then liposomes were sized by five times extrusion through a polycarbonate membrane filter with 100, 400 or 800 nm pores (Nucleopore, Maidstone, UK). For a biodistribution study, a trace amount of [³H]-CHE (74 kBq/mouse) was added to the initial chloroform solution. Particle size of PEGylated liposomes

was measured by dynamic light scattering.

2.5. Biodistribution of PEGylated liposomes

Mice were received intravenous injection of polymeric micelles (2.9 mg/kg), PEGylated liposomes (2.0 μ mol phospholipids/kg, 2.4 mg total lipids/kg) or phosphate-buffered sucrose. At three days later [³H]-labeled test-dose PEGylated liposomes (5.0 μ mol phospholipids/kg) were injected into them via a tail vein. Twenty-four hours after the test-dose administration, the mice were sacrificed for the collection of the blood from the carotid artery. Then the blood treated with heparin was centrifugally separated to obtain the plasma. After the blood was withdrawn, the heart, the lung, the liver, the spleen and the kidney were removed and weighed. The radioactivity in plasma and each organ was determined with a liquid scintillation counter (LSC-3100, Aloka, Tokyo, Japan). Distribution data are presented as % dose per wet tissue. The total amount in plasma was calculated based on the average body weight of the mice, where the average plasma volume was assumed to be 4.27% of the body weight based on the data on total blood volume.

2.6. Statistics

Variance in a group was evaluated by the *F*-test, and differences in biodistribution data, by Student's *t*-test.

3. Results and discussion

At first, we used PEGylated liposomes with 119, 261 or 795 nm diameter as a preconditioning dose. Fig. 1 shows the biodistribution of test-dose PEGylated liposomes (127 nm). The amount of the PEGylated liposomes in the plasma was significantly decreased and that in the liver was significantly increased in the mice preadministered with the PEGylated liposomes. ABC phenomenon was caused by all liposomes tested. Fig. 2 shows the biodistribution of test-dose PEGylated liposomes in the mice preadministered with polymeric micelles (9.7, 31.5 or 50.2 nm) at 3 days before. The mice prereceived

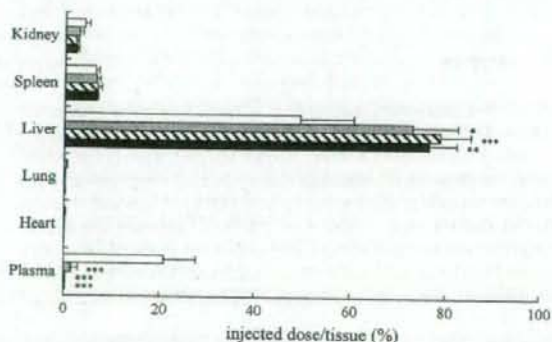
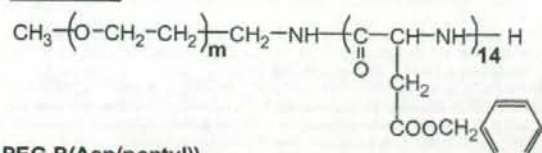


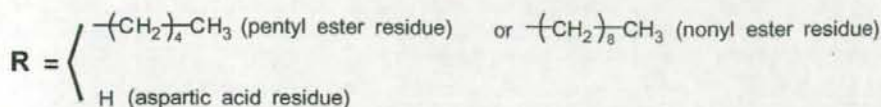
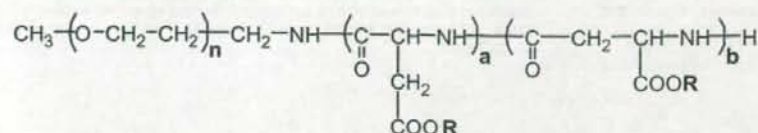
Fig. 1. Biodistribution of test-dose PEGylated liposomes after preadministration of various sized ones. BALB/c mice were intravenously injected with PEGylated liposomes (2.0 μ mol phospholipids/kg) with 119, 261 or 795 nm size. Three days later [³H]-labeled test-dose PEGylated liposomes (5.0 μ mol phospholipids/kg) were administered via a tail vein. Twenty-four hours later, the mice were sacrificed and the radioactivity in the plasma and each organ was determined (*n* = 5). Data are presented as a percentage of the injected dose per tissue and S.D. Data represent phosphate-buffered sucrose (open bar), 119 nm (gray bar), 261 nm (hatched bar), and 795 nm (closed bar) PEGylated liposomes, respectively. Significant differences against phosphate-buffered sucrose group are shown with asterisks: **p* < 0.05; ***p* < 0.01; ****p* < 0.001.

Table 1
Composition of block copolymers

PEG-PBLA



PEG-P(Asp(pentyl))
and PEG-P(Asp(nonyl))



Copolymer	Molecular weight (M.W.)	M.W. of PEG block	Number of Asp units (a + b)	Esterification degree (%) ^a	Diameter (nm) ^b
PEG-PBLA	15,000	12,000	14	100	50.2
PEG-P(Asp(pentyl))	9,000	5,000	22	75	31.5
PEG-P(Asp(nonyl))	10,000	5,000	22	72	9.7

^a Esterification degree (%) = (number of ester residues)/(number of ester residues + (number of aspartic acid residues) × 100). This degree was determined by ¹H NMR measurements.

^b Weight-weighted average diameter determined by dynamic light scattering.

50.2 nm polymeric micelles showed a significant decrease of test-dose PEGylated liposomes in the plasma and a significant increase in hepatic uptake. However, the preadministration of both 9.7 and 31.5 nm polymeric micelles did not change plasma concentration and hepatic uptake of test-dose PEGylated liposomes. It appears that ABC phenomenon was not caused by preadministration with smaller-sized polymeric micelles (31.5 nm or less), while it was triggered by preadministration with larger-sized polymeric micelles

(50.2 nm or more). These results indicate that ABC phenomenon was triggered by preconditioning with not only PEGylated liposomes but also PEG-containing polymeric micelles. Furthermore, the size of nanoassemblies presenting PEG moiety on their surface is one of important factors to induce the ABC phenomenon. In case of large particles, they would be recognized easily by immune cells and activate immune systems, presumably in spleen (Ishida et al., 2006b). By contrast, small particles might avoid the recognition by immune cells. In the point of the molecular weight of PEG moiety, we previously reported that elongation of PEG chain length did not show any difference for inducing ABC phenomenon (Ishida et al., 2005). Consequently, the larger particles may produce anti-PEG IgM (Wang et al., 2007) that triggers enhanced blood clearance and hepatic uptake of test-dose PEGylated liposomes, although further investigation should be required to prove this assumption.

4. Conclusions

This study is the first report to demonstrate that the preconditioning with polymeric micelles sized at around 50 nm, which are most widely used to deliver anti-cancer drug, causes the ABC phenomenon. Furthermore, it is clarified that the size of nanoassemblies is one of important factors for ABC phenomenon. Since nanocarriers are now progressing in the field of DDS, this study points out the important information about unexpected immune reactions against nanocarriers.

References

- Allen, T.M., Hansen, C.B., 1991. Pharmacokinetics of stealth versus conventional liposomes: effect of dose. *Biochim. Biophys. Acta* 1068, 133–141.
- Gaucher, G., Dufresne, M.H., Sant, V.P., Kang, N., Maysinger, D., Leroux, J.C., 2005. Block copolymer micelles: preparation, characterization and application in drug delivery. *J. Control. Release* 109, 169–188.

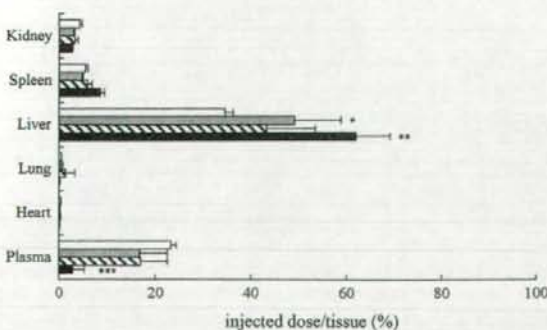


Fig. 2. Biodistribution of test-dose PEGylated liposomes after preadministration of various size polymeric micelles. BALB/c mice were intravenously injected with polymeric micelles (2.9 mg/kg) with 9.7, 31.5 or 50.2 nm size. Three days later [³H]-labeled PEGylated test-dose liposomes (5.0 μmol phospholipids/kg) were administered via a tail vein. Twenty-four hours later, the mice were sacrificed and the radioactivity in the plasma and each organ was determined (n = 5). Data are presented as a percentage of the injected dose per tissue and S.D. Data represent phosphate-buffered sucrose (open bar), 9.7 nm (gray bar), 31.5 nm (hatched bar), and 50.2 nm (closed bar) polymeric micelles, respectively. Significant differences against phosphate-buffered sucrose group are shown with asterisks: *p < 0.05; **p < 0.01; ***p < 0.001.

- Ishida, T., Harada, M., Wang, X.Y., Ichihara, M., Irimura, K., Kiwada, H., 2005. Accelerated blood clearance of PEGylated liposomes following preceding liposome injection: effects of lipid dose and PEG surface-density and chain length of the first-dose liposomes. *J. Control. Release* 105, 305–317.
- Ishida, T., Atobe, K., Wang, X., Kiwada, H., 2006a. Accelerated blood clearance of PEGylated liposomes upon repeated injections: effect of doxorubicin encapsulation and high-dose first injection. *J. Control. Release* 115, 251–258.
- Ishida, T., Ichihara, M., Wang, X., Kiwada, H., 2006b. Spleen plays an important role in the induction of accelerated blood clearance of PEGylated liposomes. *J. Control. Release* 115, 243–250.
- Ishida, T., Ichihara, M., Wang, X., Yamamoto, K., Kimura, J., Majima, E., Kiwada, H., 2006c. Injection of PEGylated liposomes in rats elicits PEG specific IgM, which is responsible for rapid elimination of a second dose of PEGylated liposomes. *J. Control. Release* 112, 15–25.
- Kwon, G.S., Kataoka, K., 1995. Block copolymer micelles as long-circulating drug vehicles. *Adv. Drug Deliv. Rev.* 16, 295–301.
- Lasic, D.D., 1996. Doxorubicin in sterically stabilized liposomes. *Nature* 380, 561–562.
- Maeda, N., Takeuchi, Y., Takada, M., Sadzuka, Y., Namba, Y., Oku, N., 2004. Anti-neovascular therapy by use of tumor neovasculature-targeted long-circulating liposome. *J. Control. Release* 100, 41–52.
- Sakakibara, T., Chen, F.A., Kida, H., Kunieda, K., Cuenca, R.E., Martin, F.A., Bankert, R.B., 1996. Doxorubicin encapsulated in sterically stabilized liposomes is superior to free drug or drug-containing conventional liposomes at suppressing growth and metastases of human lung tumor xenografts. *Cancer Res.* 56, 3743–3746.
- Wang, X., Ishida, T., Kiwada, H., 2007. Anti-PEG IgM elicited by injection of liposomes is involved in the enhanced blood clearance of a subsequent dose of PEGylated liposomes. *J. Control. Release* 119, 236–244.
- Yamamoto, T., Yokoyama, M., Opanasopit, P., Hayama, A., Kawano, K., Maitani, Y., 2007. What are determining factors for stable drug incorporation into polymeric micelle carriers? Consideration on physical and chemical characters of the micelle inner core. *J. Control. Release* 123, 11–18.
- Yokoyama, M., Kwon, G.S., Okano, T., Sakurai, Y., Seto, T., Kataoka, K., 1992. Preparation of micelle-forming polymer-drug conjugates. *Bioconjugate Chem.* 3, 295–301.
- Yokoyama, M., Okano, T., Sakurai, Y., Ekimoto, H., Shibasaki, C., Kataoka, K., 1991. Toxicity and antitumor activity against solid tumors of micelle-forming polymeric anticancer drug and its extremely long circulation in blood. *Cancer Res.* 51, 3229–3236.